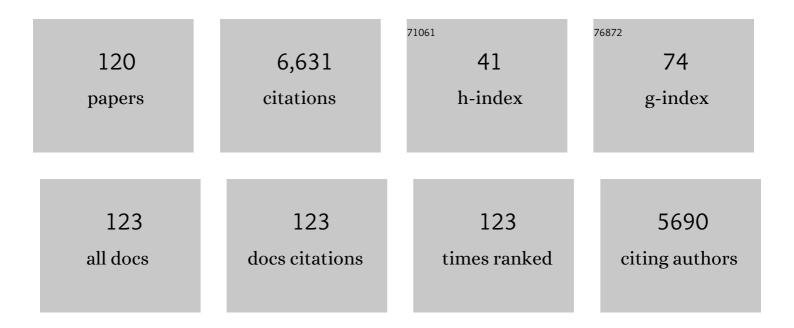
## Thao D Nguyen

List of Publications by Year in descending order

Source: https://exaly.com/author-pdf/2543974/publications.pdf Version: 2024-02-01



#	Article	IF	CITATIONS
1	Self-Folding Thermo-Magnetically Responsive Soft Microgrippers. ACS Applied Materials & Interfaces, 2015, 7, 3398-3405.	4.0	499
2	Finite deformation thermo-mechanical behavior of thermally induced shape memory polymers. Journal of the Mechanics and Physics of Solids, 2008, 56, 1730-1751.	2.3	357
3	A thermoviscoelastic model for amorphous shape memory polymers: Incorporating structural and stress relaxation. Journal of the Mechanics and Physics of Solids, 2008, 56, 2792-2814.	2.3	351
4	DNA sequence–directed shape change of photopatterned hydrogels via high-degree swelling. Science, 2017, 357, 1126-1130.	6.0	331
5	Biomechanics of the Human Posterior Sclera: Age- and Glaucoma-Related Changes Measured Using Inflation Testing. , 2012, 53, 1714.		286
6	A versatile pH sensitive chondroitin sulfate–PEG tissue adhesive and hydrogel. Biomaterials, 2010, 31, 2788-2797.	5.7	280
7	Bioâ€Origami Hydrogel Scaffolds Composed of Photocrosslinked PEG Bilayers. Advanced Healthcare Materials, 2013, 2, 1142-1150.	3.9	210
8	Full-field deformation of bovine cornea under constrained inflation conditions. Biomaterials, 2008, 29, 3896-3904.	5.7	155
9	Scleral structure and biomechanics. Progress in Retinal and Eye Research, 2020, 74, 100773.	7.3	153
10	Quantitative Mapping of Collagen Fiber Orientation in Non-glaucoma and Glaucoma Posterior Human Sclerae. , 2012, 53, 5258.		138
11	Functional stimuli responsive hydrogel devices by self-folding. Smart Materials and Structures, 2014, 23, 094008.	1.8	137
12	Modeling the Relaxation Mechanisms of Amorphous Shape Memory Polymers. Advanced Materials, 2010, 22, 3411-3423.	11.1	128
13	Scleral anisotropy and its effects on the mechanical response of the optic nerve head. Biomechanics and Modeling in Mechanobiology, 2013, 12, 941-963.	1.4	119
14	Stress-controlled viscoelastic tensile response of bovine cornea. Journal of Biomechanics, 2007, 40, 2367-2376.	0.9	118
15	Full-field bulge test for planar anisotropic tissues: Part I – Experimental methods applied to human skin tissue. Acta Biomaterialia, 2013, 9, 5913-5925.	4.1	108
16	Modeling the glass transition of amorphous networks for shape-memory behavior. Journal of the Mechanics and Physics of Solids, 2013, 61, 1612-1635.	2.3	106
17	Dual-Gel 4D Printing of Bioinspired Tubes. ACS Applied Materials & Interfaces, 2019, 11, 8492-8498.	4.0	100
18	Collagen Structure and Mechanical Properties of the Human Sclera: Analysis for the Effects of Age. Journal of Biomechanical Engineering, 2015, 137, 041006.	0.6	99

#	Article	IF	CITATIONS
19	Studies of Scleral Biomechanical Behavior Related to Susceptibility for Retinal Ganglion Cell Loss in Experimental Mouse Glaucoma. , 2013, 54, 1767.		89
20	Full-field bulge test for planar anisotropic tissues: Part II – A thin shell method for determining material parameters and comparison of two distributed fiber modeling approaches. Acta Biomaterialia, 2013, 9, 5926-5942.	4.1	83
21	Modeling the anisotropic finite-deformation viscoelastic behavior of soft fiber-reinforced composites. International Journal of Solids and Structures, 2007, 44, 8366-8389.	1.3	81
22	Glaucoma-related Changes in the Mechanical Properties and Collagen Micro-architecture of the Human Sclera. PLoS ONE, 2015, 10, e0131396.	1.1	80
23	Solvent-driven temperature memory and multiple shape memory effects. Soft Matter, 2015, 11, 3977-3985.	1.2	80
24	Viscoelastic effects on electromechanical instabilities in dielectric elastomers. Soft Matter, 2013, 9, 1031-1042.	1.2	79
25	A Nonlinear Anisotropic Viscoelastic Model for the Tensile Behavior of the Corneal Stroma. Journal of Biomechanical Engineering, 2008, 130, 041020.	0.6	78
26	An inverse finite element method for determining the anisotropic properties of the cornea. Biomechanics and Modeling in Mechanobiology, 2011, 10, 323-337.	1.4	75
27	Experimental scleral cross-linking increases glaucoma damage in a mouse model. Experimental Eye Research, 2014, 128, 129-140.	1.2	75
28	Modeling Shape-Memory Behavior of Polymers. Polymer Reviews, 2013, 53, 130-152.	5.3	74
29	The pressure-induced deformation response of the human lamina cribrosa: Analysis of regional variations. Acta Biomaterialia, 2017, 53, 123-139.	4.1	68
30	The inflation response of the posterior bovine sclera. Acta Biomaterialia, 2010, 6, 4327-4335.	4.1	67
31	The in vitro inflation response of mouse sclera. Experimental Eye Research, 2010, 91, 866-875.	1.2	67
32	Modeling the solvent-induced shape-memory behavior of glassy polymers. Soft Matter, 2013, 9, 9455.	1.2	65
33	An effective temperature theory for the nonequilibrium behavior of amorphous polymers. Journal of the Mechanics and Physics of Solids, 2015, 82, 62-81.	2.3	64
34	Indirect traumatic optic neuropathy. Military Medical Research, 2016, 3, 2.	1.9	60
35	A material force method for inelastic fracture mechanics. Journal of the Mechanics and Physics of Solids, 2005, 53, 91-121.	2.3	59
36	Influence of thermoviscoelastic properties and loading conditions on the recovery performance of shape memory polymers. Mechanics of Materials, 2011, 43, 127-138.	1.7	57

#	Article	IF	CITATIONS
37	Modeling the multiple shape memory effect and temperature memory effect in amorphous polymers. RSC Advances, 2015, 5, 416-423.	1.7	50
38	Biomechanical Responses of Lamina Cribrosa to Intraocular Pressure Change Assessed by Optical Coherence Tomography in Glaucoma Eyes. , 2017, 58, 2566.		50
39	Losartan Treatment Protects Retinal Ganglion Cells and Alters Scleral Remodeling in Experimental Glaucoma. PLoS ONE, 2015, 10, e0141137.	1.1	50
40	Viscoelasticity of the polydomain-monodomain transition in main-chain liquid crystal elastomers. Polymer, 2016, 98, 165-171.	1.8	49
41	Effect of physical aging on the shape-memory behavior of amorphous networks. Polymer, 2012, 53, 2453-2464.	1.8	46
42	Partially constrained recovery of (meth)acrylate shapeâ€memory polymer networks. Journal of Applied Polymer Science, 2012, 126, 72-82.	1.3	45
43	The effects of glycosaminoglycan degradation on the mechanical behavior of the posterior porcine sclera. Acta Biomaterialia, 2015, 12, 195-206.	4.1	45
44	Mice with an induced mutation in collagen 8A2 develop larger eyes and are resistant to retinal ganglion cell damage in an experimental glaucoma model. Molecular Vision, 2012, 18, 1093-106.	1.1	43
45	A computational model of blast loading on the human eye. Biomechanics and Modeling in Mechanobiology, 2014, 13, 123-140.	1.4	42
46	Impact of shape-memory programming on mechanically-driven recovery in polymers. Polymer, 2011, 52, 4947-4954.	1.8	41
47	In vivo characterization of the deformation of the human optic nerve head using optical coherence tomography and digital volume correlation. Acta Biomaterialia, 2019, 96, 385-399.	4.1	41
48	Depth-Dependent Changes in Collagen Organization in the Human Peripapillary Sclera. PLoS ONE, 2015, 10, e0118648.	1.1	41
49	Changes in Scleral Collagen Organization in Murine Chronic Experimental Glaucoma. , 2014, 55, 6554.		40
50	The contribution of glycosaminoglycans to the mechanical behaviour of the posterior human sclera. Journal of the Royal Society Interface, 2016, 13, 20160367.	1.5	39
51	The presence and distribution of elastin in the posterior and retrobulbar regions of the mouse eye. Experimental Eye Research, 2010, 90, 210-215.	1.2	34
52	The inflation response of the human lamina cribrosa and sclera: Analysis of deformation and interaction. Acta Biomaterialia, 2020, 106, 225-241.	4.1	34
53	Effects of Age and Diabetes on Scleral Stiffness. Journal of Biomechanical Engineering, 2015, 137, .	0.6	33
54	Artificial Intelligence Classification of Central Visual Field Patterns in Glaucoma. Ophthalmology, 2020, 127, 731-738.	2.5	33

Thao D Nguyen

#	Article	IF	CITATIONS
55	Minimal Preconditioning Effects Observed for Inflation Tests of Planar Tissues. Journal of Biomechanical Engineering, 2013, 135, 114502.	0.6	32
56	Collagen network strengthening following cyclic tensile loading. Interface Focus, 2016, 6, 20150088.	1.5	32
57	Measuring Deformation in the Mouse Optic Nerve Head and Peripapillary Sclera. , 2017, 58, 721.		32
58	A predictive parameter for the shape memory behavior of thermoplastic polymers. Journal of Polymer Science, Part B: Polymer Physics, 2016, 54, 1405-1414.	2.4	31
59	Quantification of collagen fiber structure using second harmonic generation imaging and twoâ€dimensional discrete Fourier transform analysis: Application to the human optic nerve head. Journal of Biophotonics, 2019, 12, e201800376.	1.1	31
60	Unique Recovery Behavior in Amorphous Shapeâ€Memory Polymer Networks. Macromolecular Materials and Engineering, 2012, 297, 1160-1166.	1.7	30
61	Susceptibility to glaucoma damage related to age and connective tissue mutations in mice. Experimental Eye Research, 2014, 119, 54-60.	1.2	27
62	Biomechanical assessment in models of glaucomatous optic neuropathy. Experimental Eye Research, 2015, 141, 125-138.	1.2	27
63	Synergistic Energy Absorption Mechanisms of Architected Liquid Crystal Elastomers. Advanced Materials, 2022, 34, e2200272.	11.1	27
64	A comparison of 2D and 3D digital image correlation for a membrane under inflation. Optics and Lasers in Engineering, 2016, 77, 92-99.	2.0	26
65	The Effects of Glaucoma on the Pressure-Induced Strain Response of the Human Lamina Cribrosa. , 2020, 61, 41.		25
66	Effectiveness of eye armor during blast loading. Biomechanics and Modeling in Mechanobiology, 2015, 14, 1227-1237.	1.4	24
67	Micromechanical Modeling Study of Mechanical Inhibition of Enzymatic Degradation of Collagen Tissues. Biophysical Journal, 2015, 109, 2689-2700.	0.2	23
68	Characterizing the Collagen Network Structure and Pressure-Induced Strains of the Human Lamina Cribrosa. , 2019, 60, 2406.		23
69	Effects of Geometry on the Mechanics and Alignment of Three-Dimensional Engineered Microtissues. ACS Biomaterials Science and Engineering, 2019, 5, 3843-3855.	2.6	23
70	In Situ Measurement of the Toughness of the Interface Between a Thermal Barrier Coating and a Ni Alloy. Journal of the American Ceramic Society, 2011, 94, s120.	1.9	22
71	The Temperature-Dependent Viscoelastic Behavior of Dielectric Elastomers. Journal of Applied Mechanics, Transactions ASME, 2015, 82, .	1.1	22
72	Electrostatically Driven Creep in Viscoelastic Dielectric Elastomers. Journal of Applied Mechanics, Transactions ASME, 2014, 81, .	1.1	21

#	Article	IF	CITATIONS
73	Pressure-Induced Changes in Astrocyte GFAP, Actin, and Nuclear Morphology in Mouse Optic Nerve. , 2020, 61, 14.		20
74	A nonlinear viscoelasticity theory for nematic liquid crystal elastomers. Journal of the Mechanics and Physics of Solids, 2022, 163, 104829.	2.3	20
75	A rate-dependent cohesive continuum model for the study of crack dynamics. Computer Methods in Applied Mechanics and Engineering, 2004, 193, 3239-3265.	3.4	19
76	Damping behavior of 3D woven metallic lattice materials. Scripta Materialia, 2015, 106, 1-4.	2.6	19
77	Numerical study of geometric constraint and cohesive parameters in steady-state viscoelastic crack growth. International Journal of Fracture, 2006, 141, 255-268.	1.1	18
78	Bidirectional and biaxial curving of thermoresponsive bilayer plates with soft and stiff segments. Extreme Mechanics Letters, 2017, 16, 6-12.	2.0	18
79	Modeling energy storage and structural evolution during finite viscoplastic deformation of glassy polymers. Physical Review E, 2017, 95, 063001.	0.8	18
80	Periodic buckling of soft 3D printed bioinspired tubes. Extreme Mechanics Letters, 2019, 30, 100514.	2.0	18
81	Micromechanical models for the stiffness and strength of UHMWPE macrofibrils. Journal of the Mechanics and Physics of Solids, 2018, 116, 70-98.	2.3	17
82	The Contribution of Sulfated Glycosaminoglycans to the Inflation Response of the Human Optic Nerve Head. , 2018, 59, 3144.		17
83	A thermodynamic modeling approach for dynamic softening in glassy amorphous polymers. Extreme Mechanics Letters, 2016, 8, 70-77.	2.0	16
84	Age-Related Changes in Quantitative Strain of Mouse Astrocytic Lamina Cribrosa and Peripapillary Sclera Using Confocal Microscopy in an Explant Model. , 2018, 59, 5157.		16
85	Biomimetic human small muscular pulmonary arteries. Science Advances, 2020, 6, eaaz2598.	4.7	16
86	Biomechanical Evaluations of Ocular Injury Risk for Blast Loading. Journal of Biomechanical Engineering, 2017, 139, .	0.6	15
87	Modeling the Thermoviscoelastic Properties and Recovery Behavior of Shape Memory Polymer Composites. Journal of Applied Mechanics, Transactions ASME, 2014, 81, .	1.1	14
88	A Dynamic Inflation Test for Soft Materials. Experimental Mechanics, 2016, 56, 759-769.	1.1	14
89	The effect of alignment on the rate-dependent behavior of a main-chain liquid crystal elastomer. Soft Matter, 2020, 16, 8782-8798.	1.2	14
90	A micromechanical model for the growth of collagenous tissues under mechanics-mediated collagen deposition and degradation. Journal of the Mechanical Behavior of Biomedical Materials, 2019, 98, 96-107.	1.5	13

#	ARTICLE	IF	CITATIONS
91	General Finite-Element Framework of the Virtual Fields Method in Nonlinear Elasticity. Journal of Elasticity, 2021, 145, 265-294.	0.9	13
92	Biomechanics of the optic nerve head and peripapillary sclera in a mouse model of glaucoma. Journal of the Royal Society Interface, 2020, 17, 20200708.	1.5	13
93	Regional Differences and Physiologic Behaviors in Peripapillary Scleral Fibroblasts. , 2021, 62, 27.		12

Tissue Engineering: Bioâ€Origami Hydrogel Scaffolds Composed of Photocrosslinked PEG Bilayers (Adv.) Tj ETQq0 0.0 rgBT /Overlock 10

95	Extending the effective temperature model to the large strain hardening behavior of glassy polymers. Journal of the Mechanics and Physics of Solids, 2021, 146, 104175.	2.3	11
96	The Strain Response to Intraocular Pressure Decrease in the Lamina Cribrosa of Patients with Glaucoma. Ophthalmology Glaucoma, 2023, 6, 11-22.	0.9	10
97	Thermo-mechanics of Amorphous Shape-memory Polymers. Procedia IUTAM, 2015, 12, 154-161.	1.2	9
98	On the flexural and extensional behavior of a large-tow triaxial braided composite. Composites Science and Technology, 2000, 60, 2989-2999.	3.8	8
99	Increased stiffness of collagen fibrils following cyclic tensile loading. Journal of the Mechanical Behavior of Biomedical Materials, 2018, 82, 345-354.	1.5	8
100	Biomechanics of the Cornea and Sclera. , 2016, , 285-315.		5
101	Mechanical strain in the mouse astrocytic lamina increases after exposure to recombinant trypsin. Acta Biomaterialia, 2023, 163, 312-325.	4.1	4
102	Nanoindentation of Compliant Substrate Systems: Effects of Geometry and Compliance. Journal of Engineering Materials and Technology, Transactions of the ASME, 2010, 132, .	0.8	3
103	Estimations of the effective Young's modulus of specimens prepared by fused filament fabrication. Additive Manufacturing, 2021, 42, 101983.	1.7	3
104	Effectiveness of Eye Armor During Blast Loading. , 2013, , .		2
105	Modeling the Anisotropic Finite-Deformation Viscoelastic Behavior of Soft Fiber-Reinforced Tissues. , 2007, , .		1
106	A Thermoviscoelastic Approach for Modeling Shape Memory Polymers. Materials Research Society Symposia Proceedings, 2009, 1190, 19.	0.1	1
107	Regional Variations in the Mechanical Strains of the Human Optic Nerve Head. Conference Proceedings of the Society for Experimental Mechanics, 2017, , 119-127.	0.3	1

108 The Biomechanical Response of Normal and Glaucoma Human Sclera. , 2010, , .

#	Article	IF	CITATIONS
109	The Scleral Inflation Response of Mouse Eyes to Increases in Pressure. Conference Proceedings of the Society for Experimental Mechanics, 2011, , 87-92.	0.3	1
110	On the Elastic-Plastic Response of a Large-Tow Triaxially Braided Composite. Journal of Thermoplastic Composite Materials, 2003, 16, 183-191.	2.6	0
111	Modeling the Inflation Response of C57BL/6 Mouse Sclera. , 2011, , .		0
112	Modeling the Anisotropic Properties of Human Skin Tissues. , 2012, , .		0
113	A Significant Advance in the Biomechanical Evaluation of the Optic Nerve Head. , 2014, 55, 215.		0
114	Modeling the Finite Deformation Anisotropic Viscoelastic Behavior of the Cornea. , 2008, , .		0
115	The Bulge Inflation Response of Bovine Sclera. , 2009, , .		0
116	The Inflation Response of Mouse Sclera: Age Effects on the Mechanical Properties of Scleral Tissue. , 2010, , .		0
117	Effects of the Scleral Collagen Structure on the Biomechanical Response of the Optic Nerve Head. , 2012, , .		0
118	Modeling Study Incorporating Depth-Dependent Transverse Reinforcement due to Variation in Collagen Lamellae Interweaving in Corneal Tissue. , 2012, , .		0
119	Comparing 2D and 3D Digital Image Correlation for an Inflation Test. Conference Proceedings of the Society for Experimental Mechanics, 2016, , 61-67.	0.3	0
120	Developing and characterizing human biomimetic arteriole for studying pulmonary hypertension. FASEB Journal, 2018, 32, 568.16.	0.2	0